Original Article | Gastrointestinal Imaging

eISSN 2005-8330
https://doi.org/10.3348/kjr.2019.0363
Korean J Radiol 2019;20(12):1616-1626

Korean Journal of Radiology
KJR

Intraindividual Comparison between Gadoxetate-Enhanced Magnetic Resonance Imaging and Dynamic Computed Tomography for Characterizing Focal Hepatic Lesions: A Multicenter, Multireader Study

Chansik An, MD[1], Chang Hee Lee, MD[2], Jae Ho Byun, MD[3], Min Hee Lee, MD[4], Woo Kyoung Jeong, MD[5], Sang Hyun Choi, MD[3], Do Young Kim, MD[6], Young-Suk Lim, MD[7], Young Seok Kim, MD[8], Ji Hoon Kim, MD[9], Moon Seok Choi, MD[10], Myeong-Jin Kim, MD[1]

[1]Department of Radiology, Research Institute of Radiological Science, Severance Hospital, Yonsei University College of Medicine, Seoul, Korea; Departments of [2]Radiology and [9]Internal Medicine, Korea University Guro Hospital, Korea University College of Medicine, Seoul, Korea; [3]Department of Radiology and Research Institute of Radiology, University of Ulsan College of Medicine, Asan Medical Center, Seoul, Korea; Departments of [4]Radiology and [8]Internal Medicine, Soonchunhyang University Bucheon Hospital, Bucheon, Korea; Departments of [5]Radiology and [10]Medicine, Samsung Medical Center, Sungkyunkwan University School of Medicine, Seoul, Korea; [6]Department of Internal Medicine, Severance Hospital, Yonsei University College of Medicine, Seoul, Korea; [7]Department of Internal Medicine, University of Ulsan College of Medicine, Asan Medical Center, Seoul, Korea

Objective: To compare the diagnostic accuracy of dynamic computed tomography (CT) and gadoxetate-enhanced magnetic resonance imaging (MRI) for characterization of hepatic lesions by using the Liver Imaging Reporting and Data System (LI-RADS) in a multicenter, off-site evaluation.

Materials and Methods: In this retrospective multicenter study, we evaluated 231 hepatic lesions (114 hepatocellular carcinomas [HCCs], 58 non-HCC malignancies, and 59 benign lesions) confirmed histologically in 217 patients with chronic liver disease who underwent both gadoxetate-enhanced MRI and dynamic CT at one of five tertiary hospitals. Four radiologists at different institutes independently reviewed all MR images first and the CT images 4 weeks later. They evaluated the major and ancillary imaging features and categorized each hepatic lesion according to the LI-RADS v2014. Diagnostic performance was calculated and compared using generalized estimating equations.

Results: MRI showed higher sensitivity and accuracy than CT for diagnosing hepatic malignancies; the pooled sensitivities, specificities, and accuracies for categorizing LR-5/5V/M were 59.0% vs. 72.4% (CT vs. MRI; $p < 0.001$), 83.5% vs. 83.9% ($p = 0.906$), and 65.3% vs. 75.3% ($p < 0.001$), respectively. CT and MRI showed comparable capabilities for differentiating between HCC and other malignancies, with pooled accuracies of 79.9% and 82.4% for categorizing LR-M, respectively ($p = 0.139$).

Conclusion: Gadoxetate-enhanced MRI showed superior accuracy for categorizing LR-5/5V/M in hepatic malignancies in comparison with dynamic CT. Both modalities had comparable accuracies for distinguishing other malignancies from HCC.

Keywords: *Hepatocellular carcinoma; Magnetic resonance imaging; Computed tomography; Contrast media; Data systems; Gadolinium ethoxybenzyl DTPA*

Received May 29, 2019; accepted after revision August 15, 2019.
This study was supported by a grant from Bayer Korea Ltd.

Corresponding author: Myeong-Jin Kim, MD, Department of Radiology, Research Institute of Radiological Science, Severance Hospital, Yonsei University College of Medicine, 50-1 Yonsei-ro, Seodaemun-gu, Seoul 03722, Korea.
• Tel: (822) 2228-7400 • Fax: (822) 393-3035 • E-mail: kimnex@yuhs.ac

Korean Journal of Radiology
KJR

INTRODUCTION

Current guidelines for the management of hepatocellular carcinoma (HCC) allow the diagnosis of HCC in high-risk patients without histologic confirmation if a hepatic lesion shows typical findings on dynamic contrast-enhanced computed tomography (CT) or magnetic resonance imaging (MRI) (1-5). However, non-HCC malignancies such as intrahepatic cholangiocarcinoma (CCA) or combined HCC-CCA may also display imaging findings of typical HCCs, particularly in small tumors in the cirrhotic liver (6-8). Since the treatment options and prognoses are different for non-HCC malignancies and HCC, imaging-based differentiation of HCC and other malignancies is important (9, 10).

The Liver Imaging Reporting and Data System (LI-RADS), unlike other diagnostic criteria, addresses the issue of imaging diagnosis of non-HCC malignancies (11, 12). It requires the LR-M category to be assigned to a hepatic lesion suspected to be a non-HCC malignancy, and recommends histological diagnosis of these LR-M lesions (13, 14).

Although previous studies have compared the LI-RADS diagnostic accuracy of gadoxetate-enhanced MRI and dynamic CT (15-18), a multicenter study involving off-site evaluations by multiple readers has not been performed. Therefore, the purpose of this study was to compare the diagnostic performance of gadoxetate-enhanced MRI and dynamic CT for assessments based on LI-RADS v2014 during characterization of focal hepatic lesions in patients with chronic liver disease.

MATERIALS AND METHODS

Subjects

This retrospective multicenter study was approved by the Institutional Review Boards of all five participating institutions, which are academic tertiary hospitals in Korea. The requirement for written informed consent for the retrospective review of medical records and image data was waived.

Investigators from five institutions searched the databases to identify patients aged 18 years or older who met the following inclusion criteria: 1) at risk of developing HCC (hepatitis B virus [HBV] carrier, hepatitis C virus carrier with chronic hepatitis, or cirrhosis from any causes), 2) pathologic diagnosis of focal hepatic lesions based on surgery or biopsy findings between January 2008 and July 2014, 3) both dynamic CT and gadoxetate-enhanced MRI performed within 2 months before the pathologic diagnosis, and 4) no past history of hepatic malignancy. Of the 2958 patients who met the inclusion criteria, 287 were excluded because they had undergone local ablative treatments (n = 274), had ruptured HCCs (n = 3), had active extrahepatic malignancy (n = 6), or had false-negative biopsy results (n = 4). From the remaining 2671 patients, 103 patients with 117 non-HCC lesions (59 benign lesions and 58 non-HCC malignancies) were included; we also randomly selected 114 patients with 114 HCCs. Our final study population consisted of 217 patients with 231 pathologically-confirmed hepatic lesions (Fig. 1).

Image Acquisition

MRI was performed using 1.5T or 3T scanners. The protocols included a dual-echo T1-weighted gradient-recalled echo sequence, moderately and heavily T2-weighted turbo spin-echo sequences, dynamic three-dimensional T1-weighted gradient-recalled echo sequence using gadoxetic acid disodium (Primovist, Bayer AG, Berlin, Germany) as

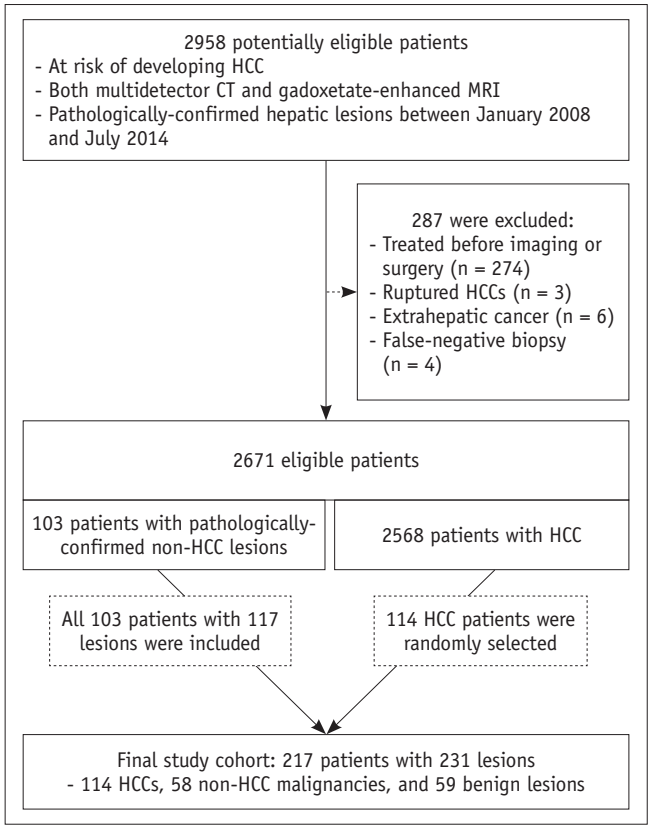

Fig. 1. Flowchart illustrating subject selection. CT = computed tomography, HCC = hepatocellular carcinoma, MRI = magnetic resonance imaging

https://doi.org/10.3348/kjr.2019.0363

the contrast medium, and diffusion-weighted imaging. For dynamic imaging, arterial-, portal venous-, transitional-, and hepatobiliary-phase images were acquired 25–35 seconds, 60–70 seconds, 2 or 3 minutes, and 15 or 20 minutes after contrast injection, respectively. Contrast-enhanced dynamic CT was performed using 16-, 40-, or 64-detector scanners. After acquiring unenhanced images, arterial-, portal venous-, and delayed-phase images were obtained approximately 30 seconds, 70 seconds or 90 seconds, and 180 seconds or 210 seconds after iodinated contrast medium injection, respectively. Technical details for CT and MRI acquisition are provided in Supplementary Material 1.

Data Collection and Preparation

Clinical, pathologic, and imaging data were retrieved from the database of each participating institution, which included information about patient demographics, the cause of chronic liver disease, serum alpha-fetoprotein level, child-Pugh class, pathologic diagnosis, and CT/MR images. They were then sent to the central site (Severance Hospital), where the image data were anonymized, randomized, and assigned new identification numbers. The processed imaging data, along with screen-captured images marking the lesions' sites (which was performed by an abdominal radiologist with 4 years of experience), were then sent back for image analysis. The data collection and preparation steps are described in detail in Supplementary Material 2.

Image Analysis

Four board-certified abdominal radiologists from different institutions (Reviewer 1, Reviewer 2, Reviewer 3, and Reviewer 4, with 5, 6, 10, and 21 years of experience, respectively, in abdominal CT and MRI) independently analyzed the CT/MR images and submitted the results to the central site. In the first round, they analyzed the MR images to evaluate the LI-RADS features and determine the initial LI-RADS category in each case without assessing the ancillary features. Then, they evaluated the ancillary features and assigned the final LI-RADS category. They did not evaluate the presence or absence of threshold growth. In the second round conducted at least 8 weeks after the first round to minimize recall bias, they evaluated the CT images in the same manner. In cases where a hepatic lesion could not be delineated in the marked area, it was recorded as "not visible" and considered benign. The washout appearance was determined twice, first as defined in the LI-RADS by using the portal venous phase alone (11, 13, 14), and then by using both portal- and transitional-phase images. The reviewers were asked to characterize a feature as absent if they could not unequivocally determine whether the feature was present or absent due to suboptimal or poor image quality.

A detailed description of the image analysis protocol is provided in Supplementary Material 3.

Statistical Analysis

For sample size estimation, the expected per-lesion sensitivities of dynamic CT and MRI for HCC were assumed to be 68% and 80%, respectively, with the same specificity of 94% (19). On the basis of these expected values and a power of 80%, we calculated that we would need 209 or more hepatic lesions to obtain a significant difference in diagnostic performance with a two-sided type I error of 5% (20).

The baseline characteristics were compared using analysis of variance for continuous variables and the chi-squared test for categorical variables. Multiple comparisons were corrected using Bonferroni's method. The frequency of image features was compared using chi-squared or Fisher's exact tests. We used a generalized estimating equation method to compare the diagnostic performance between dynamic CT and MRI for distinguishing hepatic malignancies from benign lesions categorized as LR-5, LR-5V, or LR-M; for differentiating HCC from non-HCC lesions categorized as LR-5 or LR-5V; for differentiating non-HCC malignancies from other lesions categorized as LR-M; and then in subgroups containing only two disease entities for differentiating between HCC and benign lesions (with other malignancies excluded) and between HCC and other malignancies (with benign lesions excluded). In addition, we examined the diagnostic performance of LR-5 (without LR-5V) for HCC. We used LR-5 alone, not including LR-4, for the calculation of diagnostic accuracy, because LR-5 alone is considered to indicate "definite HCC" in LI-RADS (11, 13, 14). Lastly, we calculated the diagnostic performance of gadoxetate-enhanced MRI when using the portal phase alone for washout evaluation and compared it with the results obtained using both the portal and transitional phases. Pathologic diagnosis was used as a reference standard. To examine the added value of the ancillary features, we tabulated the LI-RADS categories before and after applying the ancillary features and calculated the

https://doi.org/10.3348/kjr.2019.0363

Korean Journal of Radiology
KJR

net reclassification improvement. The net reclassification improvement is a statistic for assessing the improvement in performance gained by adding a new factor to a model by measuring the extent to which individual subjects with and without disease are appropriately reclassified into more appropriate categories (21). We performed this analysis only on MRI cases after excluding the LR-M and "not visible" cases. Kappa statistics were computed as indices of inter-reader agreements between the four readers. Kappa statistics were used to indicate agreement, with 0.8–1.0 indicating excellent agreement; 0.60–0.79, good agreement; 0.40–0.59, moderate agreement; 0.20–0.39, fair agreement; and 0–0.19, poor agreement. All statistical analyses were performed using SAS 9.2 (SAS Institute Inc., Cary, NC, USA) and R version 3.3.3 (The R Foundation for Statistical Computing, Vienna, Austria). *P* values < 0.05 were considered statistically significant. A detailed description of our statistical analysis is provided in Supplementary Material 4.

RESULTS

Baseline Characteristics, LI-RADS Categories, and Major Features

The baseline characteristics of the 217 patients with 231 hepatic lesions (114 HCCs, 58 other malignancies, and 59 benign lesions) are summarized in Table 1. Patients with other malignancies were significantly older compared to those with HCCs ($p = 0.017$) and benign lesions ($p = 0.006$). HBV was a more common etiology of chronic liver disease in patients with HCCs than in those with benign lesions ($p = 0.003$). Tumor size was the largest in patients with other malignancies and the smallest in patients with benign lesions ($p < 0.001$), and biopsy was more frequently used for the diagnosis of other malignancies or benign lesions than HCCs ($p < 0.001$). The interval between CT and MRI ranged from 0 to 64 days, with a median interval of 12 days. Pathologic diagnosis was performed within 2 months after the first imaging study as it was one of our inclusion

Table 1. Baseline Characteristics

Characteristic	HCC	OM*	Benign†	*P*	Total
Per-patient basis					
Number of patients	114	53	50		217
Median age (range, years)	59 (40–85)	63 (42–76)	55 (36–78)	0.003	59 (36–85)
Sex (%)				0.835	
Male	89 (78.1)	40 (75.5)	37 (74.0)		166 (76.5)
Female	25 (21.9)	13 (24.5)	13 (26.0)		51 (23.5)
Cause of chronic liver disease (%)				0.003	
HBV	98 (86.8)	38 (71.7)	32 (64.0)		168 (77.9)
HCV	7 (6.1)	2 (3.8)	3 (6.0)		12 (5.5)
HBV/HCV coinfection	0 (0)	1 (1.9)	0 (0)		1 (0.5)
Non-viral	9 (7.0)	12 (22.6)	15 (30.0)		36 (16.1)
Child-Pugh class (%)				0.285	
A	102 (89.5)	50 (94.3)	48 (96.0)		200 (92.2)
B	10 (8.8)	3 (5.7)	2 (4.0)		15 (6.9)
C	2 (1.7)	0 (0)	0 (0)		2 (0.9)
Median AFP (range, ng/mL)	9.35 (0.6–50676.0)	4.4 (1.3–1771.0)	3.9 (0.9–55.1)	< 0.001	5.5 (0.6–50676.0)
Per-lesion basis					
Number of lesions	114	58	59		231
Median size (range, cm)	2.3 (0.5–12.2)	2.8 (0.5–13.2)	1.5 (0.7–7.1)	< 0.001	2.1 (0.3–13.3)
Method of diagnosis (%)				< 0.001	
Biopsy	3 (2.6)	12 (20.7)	22 (37.3)		37 (16.0)
Resection	110 (96.5)	46 (79.3)	35 (59.3)		191 (82.7)
Transplantation	1 (0.9)	0 (0)	2 (3.4)		3 (1.3)

*OM includes 30 intrahepatic cholangiocarcinomas, 15 combined hepatocellular-cholangiocarcinomas, 11 metastases, 1 neuroendocrine carcinoma, and 1 lymphoepithelioma-like carcinoma, †Benign lesion includes 29 dysplastic/regenerative nodules, 8 focal nodular hyperplasia-like nodules, 8 hemangiomas, 5 angiomyolipomas, 3 bile duct adenomas, 2 adenomas, 2 eosinophilic abscesses, 1 inflammatory pseudotumor, and 1 tuberculoma. AFP = alpha-fetoprotein, HBV = hepatitis B virus, HCC = hepatocellular carcinoma, HCV = hepatitis C virus, OM = other malignancies

https://doi.org/10.3348/kjr.2019.0363

criteria.

The frequencies of HCCs, other malignancies, and benign lesions according to the LI-RADS category and imaging modality are presented in Figure 2 (only pooled results) and Supplementary Table 1 (including full results). Minor proportions of non-HCC malignancies were categorized as LR-5V (3.4% [8/232] for CT and 4.7% [11/232] for MRI) (Figs. 2, 3).

The frequencies of major features—arterial-phase hyperenhancement, washout appearance, and capsule appearance—according to imaging modality are presented in Supplementary Tables 2 (by disease) and 3 (by size, only including HCCs). There were seven cases in which at least one reviewer decided that evaluation of arterial-phase MR images was suboptimal because of severe motion artifacts or too early acquisition. In HCC lesions, diffuse arterial hyperenhancement and washout appearance either in the portal or transitional phase were more frequently observed on MRI than on CT (88.2% vs. 82.5% [p = 0.015] and 90.4% vs. 77.2% [p = 0.005], respectively), but the frequency of washout appearance observed on MRI became lower than that on CT when the washout appearance was determined in the portal phase alone (71.1% vs. 77.2% [p = 0.034]). Rim-like arterial-phase hyperenhancement, a feature favoring malignancies other than HCC, was more frequently observed on MRI than on CT in non-HCC malignancies (44.8% vs. 32.3%, p = 0.006), but not in HCC (4.6% vs. 6.8%, p = 0.205) or benign lesions (7.2% vs. 5.5%, p = 0.572).

Diagnostic Performance of Dynamic CT and MRI

Diagnosis of Hepatic Malignancies

In the diagnosis of hepatic malignancies, MRI showed higher sensitivity and accuracy than CT, but the specificities of the two methods were not significantly different (Table 2 [only pooled results], Supplementary Table 4 [including full results], and Fig. 4). With data pooled from all the reviewers, the sensitivity, specificity, and accuracy were 72.4%, 83.9%, and 75.3%, respectively, for MRI, and 59.0%, 83.5%, and 65.3%, respectively, for CT (p < 0.001 for sensitivity and accuracy, and p = 0.906 for specificity). For differentiation of HCC from non-HCC lesions, MRI showed higher sensitivity but lower specificity than CT, and accuracy was not significantly different with or without including LR-5V in the diagnostic criteria (p > 0.576). For differentiation of other malignancies from HCC and benign lesions, no significant differences were observed in sensitivity, specificity, and accuracy between CT and MRI (p = 0.139).

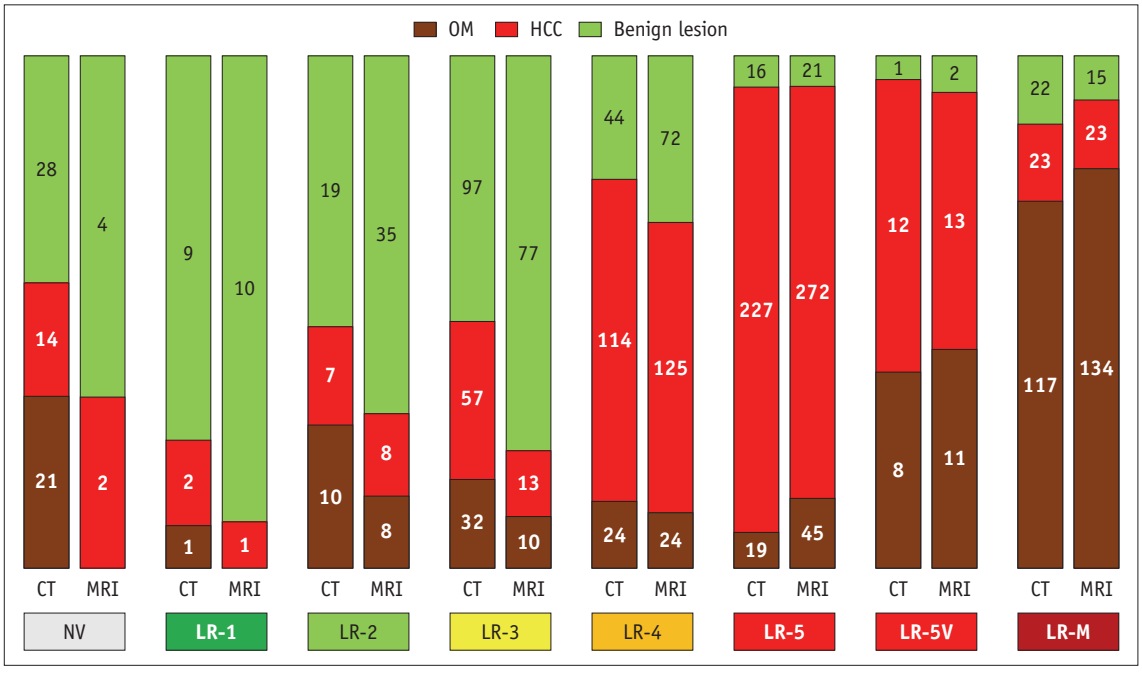

Fig. 2. Frequencies and proportions of HCC, OM, and benign lesions according to imaging modality and Liver Imaging Reporting and Data System category. Numbers and areas of segments in each vertical bar indicate numbers and proportions of HCC, OM, and benign lesions, respectively. Pooled results from four reviewers are shown here (see Supplementary Table 1 for full results). NV = not visible, OM = other malignancies

https://doi.org/10.3348/kjr.2019.0363

Korean Journal of Radiology
KJR

Analyses of Subgroups Containing Only Two Disease Entities

In a subgroup with HCC and benign lesions (other malignancies excluded), MRI showed higher sensitivity and accuracy than CT for the diagnosis of HCC (with the pooled data, 62.5% vs. 52.4% [p = 0.003] and 72.0% vs. 66.2% [p = 0.019], respectively) with similar specificities (90.3% vs. 92.8%, p = 0.352). However, in a subgroup with HCC and other malignancies (benign lesions excluded), the sensitivity, specificity, and accuracy of MRI and CT for discriminating other malignancies from HCC were not significantly different (p > 0.150) (Table 3 [only pooled results] and Supplementary Table 5 [including full results]). Similar results were obtained when LR-5V was not considered diagnostic for HCC.

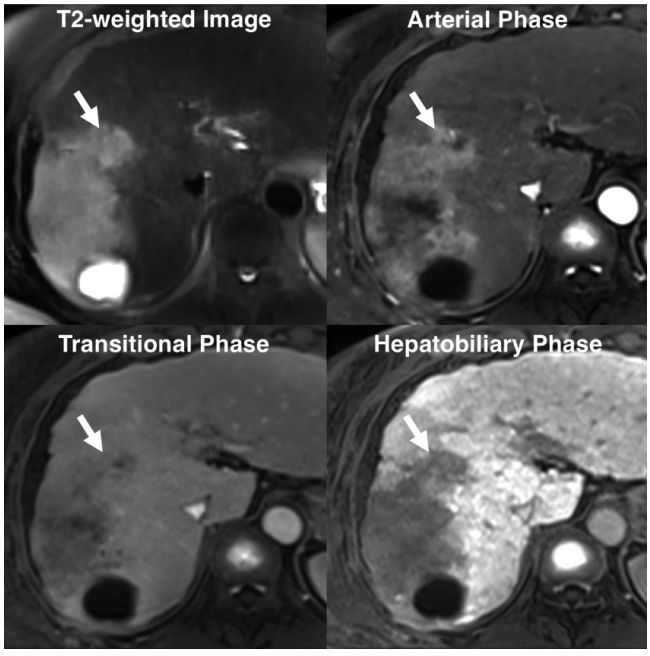

Fig. 3. Non-HCC malignancy with tumor in vein. Diffuse hypervascular tumor with infiltrative margins is seen at right hemiliver. Tumor also invades adjacent portal vein branch (P8), forming mass within vein (arrows). Two of our four reviewers categorized this mass as LR-5V, while other two assigned score of LR-M. Pathologic diagnosis obtained after biopsy was combined HCC-cholangiocarcinoma.

Comparison of the Portal and Delayed Phases for Evaluating the Washout Appearance

When the portal phase alone was used for evaluating the washout appearance, the pooled results demonstrated that the specificity significantly increased (p = 0.049) but

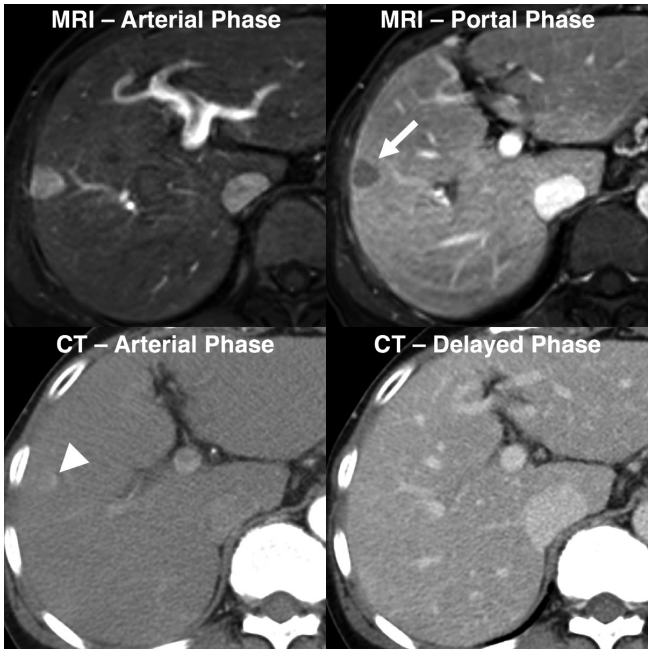

Fig. 4. Pathologically-confirmed HCC categorized as LR-5 only with gadoxetate-enhanced MRI. 58-year-old female HBV carrier underwent both dynamic CT and gadoxetate-enhanced MRI with interval of 3 days. Her serum alpha-fetoprotein level was elevated at surveillance for HCC. On gadoxetate-enhanced MRI, all our reviewers found 1.8-cm nodule in right liver (arrow) with arterial hyperenhancement, portal washout appearance, and capsule appearance, and categorized this nodule as LR-5. However, on dynamic CT, only faint arterial hyperenhancement (arrowhead) was visualized at corresponding location. All reviewers categorized lesion as LR-3 or LR-4. HBV = hepatitis B virus

Table 2. Diagnostic Performance of CT and Gadoxetate-Enhanced MRI for Hepatic Malignancy

	LR-5/5V/M for Hepatic Malignancy			LR-5/5V for HCC			LR-5 for HCC			LR-M for Non-HCC Malignancies		
	CT	MRI	*P*	CT	MRI	*P*	CT	MRI	*P*	CT	MRI	*P*
TP/TN/FP/FN	406/197/39/282	498/198/38/190		239/424/44/217	285/389/79/171		227/433/35/229	272/402/66/184		117/647/45/115	134/654/38/98	
Sensitivity, %	59.0	72.4	< 0.001	52.4	62.5	0.003	49.8	59.7	0.004	50.4	57.8	0.167
Specificity, %	83.5	83.9	0.906	90.6	83.1	0.002	92.5	85.9	0.003	93.5	94.5	0.494
Accuracy, %	65.3	75.3	< 0.001	71.8	72.9	0.576	71.4	72.9	0.468	82.7	85.3	0.139

These are pooled results from four reviewers. Unless otherwise specified, data represent numbers of cases. CT = computed tomography, FN = false negative, FP = false positive, MRI = magnetic resonance imaging, TN = true negative, TP = true positive

https://doi.org/10.3348/kjr.2019.0363

sensitivity and accuracy significantly decreased ($p < 0.002$) compared to the findings obtained using both portal and transitional phases in the diagnosis of hepatic malignancies (Table 4 [only pooled results] and Supplementary Table 6 [including full results]). However, despite the decrease in sensitivity, MRI showed significantly higher sensitivity (67.7% vs. 59.0%, $p < 0.001$) and accuracy (72.5% vs. 65.3%, $p < 0.001$) than CT (Table 4).

Added Value of the Ancillary Features in Gadoxetate-Enhanced MRI

Analysis of the pooled data revealed that the ancillary features modified the final LI-RADS category in 110 (12.0%) of 918 cases (Supplementary Table 7). None of the LR-4 cases was upgraded to LR-5, as it is not warranted by the LI-RADS (7). Of the 686 malignant cases, 22 (3.2%) were correctly upgraded into higher LI-RADS categories, while 25 (3.6%) were incorrectly downgraded into lower categories. Of the 232 benign cases, 36 (15.5%) and 28 (12.1%) were reclassified into higher and lower LI-RADS categories, respectively. The overall net reclassification improvement was estimated to be -0.055 ($p = 0.117$), indicating a negative impact on the overall categorization without statistical significance. However, of 32 and 19 benign cases initially categorized as LR-5/5V and LR-M, 10 (31.3%) and 4 (21.1%), respectively, were correctly downgraded into lower categories after applying ancillary features (Fig. 5).

Inter-Reader Agreement

When the LI-RADS categories were grouped into three categories of LR-5/5V, LR-M, and LR-1/2/3/4, inter-reader agreements were good for both CT and MRI ($\kappa = 0.626$ and 0.601, respectively). Inter-reader agreements were good for arterial hyperenhancement assessments using CT ($\kappa = 0.675$) and moderate MRI ($\kappa = 0.563$), for assessments of washout appearance by using CT and MRI ($\kappa = 0.510$ and 0.532, respectively), as well as for assessments of capsule appearance by using CT ($\kappa = 0.476$). However, inter-reader agreement was fair for assessments of capsule appearance by using MRI ($\kappa = 0.326$).

DISCUSSION

The results of this multicenter, off-site reader study showed that gadoxetate-enhanced MRI has higher sensitivity and accuracy than CT in discriminating between malignant and benign lesions in patients with chronic liver disease, as shown in previous studies (19, 22). However, other recent studies have shown that the diagnostic accuracy was comparable between gadoxetate-

Table 3. Diagnostic Performance of CT and Gadoxetate-Enhanced MRI in Differentiation of HCC from Benign Lesions and OM from HCC

	LR-5/5V for HCC vs. Benign			LR-5 for HCC vs. Benign			LR-M for HCC vs. OM		
	CT	MRI	*P*	CT	MRI	*P*	CT	MRI	*P*
TP/TN/FP/FN	239/219/17/217	285/213/23/171		227/220/16/229	272/215/21/184		117/433/23/115	134/433/23/98	
Sensitivity, %	52.4	62.5	0.003	49.8	59.7	0.005	50.4	57.8	0.167
Specificity, %	92.8	90.3	0.352	93.2	91.1	0.398	95.0	95.0	0.999
Accuracy, %	66.2	72.0	0.019	64.6	70.4	0.017	79.9	82.4	0.139

These are pooled results from four reviewers. Unless otherwise specified, data represent numbers of cases. These are results from subgroup analysis in differentiation of HCC from benign lesions (with OM excluded from analysis) and OM from HCC (with benign lesions excluded from analysis).

Table 4. Diagnostic Performance of Gadoxetate-Enhanced MRI Using PP Alone for Washout Appearnace

	(a) CT	(b) MRI Using PP and TRP	(c) MRI Using PP Alone	*P*	*P** (a) vs. (c)	*P** (b) vs. (c)
TP/TN/FP/FN	406/197/39/282	498/198/38/190	466/204/32/222			
Sensitivity, %	59.0	72.4	67.7	< 0.001	< 0.001	< 0.001
Specificity, %	83.5	83.9	86.4	0.119	0.374	0.049
Accuracy, %	65.3	75.3	72.5	< 0.001	< 0.001	0.002

These are pooled results from four reviewers. These results show diagnostic performance of gadoxetate-enhanced MRI when using portal phase alone for evaluating washout appearance, in comparison with CT or MRI using both portal and transitional phases in diangosis of hepatic malignancies. *p values from post-hoc tests. PP = portal phase, TRP = transitional phase

https://doi.org/10.3348/kjr.2019.0363

Korean Journal of Radiology
KJR

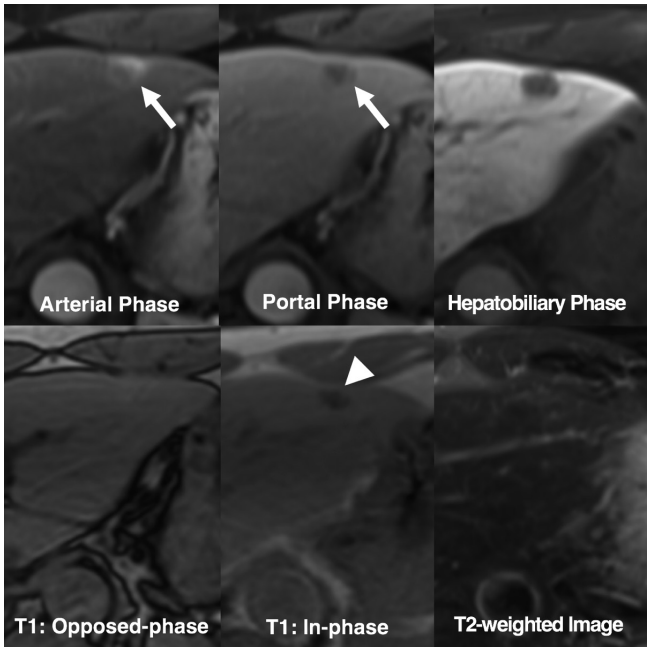

Fig. 5. Benign lesion initially categorized as LR-5 but correctly downgraded by applying ancillary features. 52-year-old HBV carrier underwent gadoxetate-enhanced MRI after hepatic nodule was found on ultrasonography. 1.4-cm nodule in left liver shows arterial hyperenhancement (arrow) and washout appearance on portal phase (arrow). Two reviewers considered arterial enhancement as rim-like and categorized nodule as LR-M. Other reviewers initially categorized nodule as LR-5. Nodule shows signal drop from opposed-phase to in-phase of T1-weighted gradient-recalled echo sequence (arrowhead), indicating presence of intralesional iron deposits. Note that nodule shows isointensity on T2-weighted image. These features are uncommon finding in progressed HCCs. After applying these ancillary features, reviewers downgraded their categories to LR-4. This nodule was confirmed as angiomyolipoma after hepatic resection.

enhanced MRI and CT for the diagnosis and characterization of hepatic lesions on the basis of LI-RADS (23-25). In comparison with our study, these results were not obtained in a multicenter study involving off-site evaluation by multiple readers. Furthermore, we included a substantial number of cases involving non-HCC malignancies because our purpose was to compare the performance of dynamic CT and MRI in differential diagnosis. Therefore, we believe that the multicenter and multireader study design as well as the addition of a sufficient number of non-HCC malignancies would be strengths of our study. The higher sensitivity of gadoxetate-enhanced MRI in differentiating hepatic lesions could be attributed to its superiority in demonstrating imaging features favoring malignancies. In line with a recently published study (26), we found that arterial hyperenhancement as well as washout appearance were more frequently observed in HCCs on gadoxetate-enhanced MRI than on CT.

In contrast, the accuracy for differentiating HCCs from other malignancies was comparable between gadoxetate-enhanced MRI and CT, as suggested by previous studies in which both gadoxetate-enhanced MRI and CT showed limitations in accurately discriminating HCC from other malignancies, especially combined HCC-CCA (27-30). Furthermore, similar to a previous report (27), we noted that 3.4% (8/232) and 4.7% (11/232) of non-HCC malignancies showed tumors in the vein and were categorized as LR-5V for CT and MRI, respectively, which further decreased the specificity of LR-5/5V for HCC diagnosis. However, the latest version (v2018) of LI-RADS has revised LR-5V (definitely HCC with tumor in vein [TIV]) to LR-TIV, so the presence of the TIV would no longer decrease the specificity for HCC diagnosis (31).

We observed that the application of the ancillary features modified the LI-RADS categories in 12% (111/924) of cases, similar to the results of two recent studies (15.3% and 18.1%) (12, 25). In our study, no significant improvement was observed in the overall LI-RADS categorization with addition of the ancillary features. However, 10 benign lesions initially categorized as LR-5/5V were correctly downgraded (Fig. 5, Supplementary Table 7). Two recent studies using extracellular contrast media reported conflicting results on the impact of upgrading LR-3 to LR-4 based on ancillary features on the diagnostic performance (12, 32). Both studies showed that the application of ancillary features increased the sensitivity of LR-4/5/5V for HCC, while the specificity was shown to be preserved in one study (12) and decreased in another (32).

Our study also showed that multicenter, off-site evaluations could achieve comparable inter-reader agreement for LI-RADS categorization with both MRI and CT, as seen in previous single-center studies (33, 34). A recent study involving 113 readers from eight different sites reported a better inter-reader agreement (35). However, in that study, preselected screen-captured images were evaluated, in contrast to our study, in which whole series of images were provided to the reviewers.

This study had limitations. First, our study may have biases due to its retrospective design. There were differences in several baseline characteristics between patients with malignant and benign lesions in this study, which might have resulted in further biases. In addition, inclusion of only pathologically-confirmed lesions may have been a source of selection bias. For example, most of the benign lesions included were likely difficult to diagnose by

https://doi.org/10.3348/kjr.2019.0363

imaging alone, which might have affected the diagnostic accuracy—most likely by underestimating the specificity. However, we believe that the reference standard for evaluating the performance during differential diagnosis of hepatic tumors must be histopathological findings, since some non-HCC malignancies may show the typical imaging features of HCCs (8, 23, 28) and these HCC mimickers can be treated by locoregional or systemic treatment without pathologic confirmation according to the current guidelines (28). Second, we used the earlier version of LI-RADS (v2014) because it was the latest version available at the time of our image analysis. However, except for the change from LR-5V to LR-TIV, only minor changes (i.e., mainly more elaborate definitions of features) have been made in the diagnostic table (12). Furthermore, we obtained similar results when only LR-5 was considered positive for HCC diagnosis. In addition, since the LI-RADS v2014 did not specifically define high-risk patients and advised to follow the other guidelines, we also included non-cirrhotic patients with chronic hepatitis C according to European Association for the Study of the Liver (2). However, the latest version (v2018) of LI-RADS does not consider chronic hepatitis C patients at risk. Thus, our loose inclusion criteria might have affected the results, although the proportion of such patients was small (i.e., about 5%). Third, we evaluated washout appearance using two methods; by using portal phase alone and also by using both portal and transitional phases. Using the transitional phase for evaluating washout appearance might have led to an overestimation of sensitivity of gadoxetate-enhanced MRI. However, we also obtained similar results in the supplementary analysis performed using the portal phase alone for washout evaluation.

In conclusion, our multicenter off-site evaluation study showed that gadoxetate-enhanced MRI was superior to CT in differentiating hepatic malignancies from benign lesions by using the LI-RADS v2014 in patients with chronic liver disease. Both modalities had comparable capabilities for distinguishing HCC and other malignancies. The ancillary features on gadoxetate-enhanced MRI may help avoid misdiagnosis of benign lesions as definitely malignant lesions.

Supplementary Materials

The Data Supplement is available with this article at https://doi.org/10.3348/kjr.2019.0363.

Conflicts of Interest

The funder Bayer Korea Ltd. had no role in the study design; the collection, analysis, and interpretation of data; the writing of the report; or the decision to submit the manuscript for publication.

Acknowledgments

The authors would like to thank Sungwon Kim, MD, Jun Tae Kim, and Kyunghwa Han, PhD, from the Department of Radiology, Yonsei University College of Medicine, for their assistance in data collection and preparation (S.K. and J.K.) and statistical analysis (K.H.).

ORCID iDs

Myeong-Jin Kim
https://orcid.org/0000-0001-7949-5402
Chansik An
https://orcid.org/0000-0002-0484-6658

REFERENCES

1. Marrero JA, Kulik LM, Sirlin CB, Zhu AX, Finn RS, Abecassis MM, et al. Diagnosis, staging, and management of hepatocellular carcinoma: 2018 practice guidance by the American Association for the Study of Liver Diseases. *Hepatology* 2018;68:723-750
2. European Association for the Study of the Liver. EASL clinical practice guidelines: management of hepatocellular carcinoma. *J Hepatol* 2018;69:182-236
3. Omata M, Cheng AL, Kokudo N, Kudo M, Lee JM, Jia J, et al. Asia-Pacific clinical practice guidelines on the management of hepatocellular carcinoma: a 2017 update. *Hepatol Int* 2017;11:317-370
4. Korean Liver Cancer Study Group and Korean National Cancer Center. 2014 Korean Liver Cancer Study Group-National Cancer Center Korea practice guideline for the management of hepatocellular carcinoma. *Korean J Radiol* 2015;16:465-522
5. Kudo M, Trevisani F, Abou-Alfa GK, Rimassa L. Hepatocellular carcinoma: therapeutic guidelines and medical treatment. *Liver Cancer* 2016;6:16-26
6. Kim YY, An C, Kim DY, Aljoqiman KS, Choi JY, Kim MJ. Failure of hepatocellular carcinoma surveillance: inadequate echogenic window and macronodular parenchyma as potential culprits. *Ultrasonography* 2019;38:311-320
7. Rhee H, Kim MJ, Park YN, An C. A proposal of imaging classification of intrahepatic mass-forming cholangiocarcinoma into ductal and parenchymal types: clinicopathologic significance. *Eur Radiol* 2019;29:3111-3121
8. Kim YY, Park MS, Aljoqiman KS, Choi JY, Kim MJ. Gadoxetic acid-enhanced magnetic resonance imaging: hepatocellular carcinoma and mimickers. *Clin Mol Hepatol* 2019;25:223-233

9. Han S, Choi JI, Park MY, Choi MH, Rha SE, Lee YJ. The diagnostic performance of liver MRI without intravenous contrast for detecting hepatocellular carcinoma: a case-controlled feasibility study. *Korean J Radiol* 2018;19:568-577
10. Murakami T, Tsurusaki M. Hypervascular benign and malignant liver tumors that require differentiation from hepatocellular carcinoma: key points of imaging diagnosis. *Liver Cancer* 2014;3:85-96
11. Chernyak V, Fowler KJ, Kamaya A, Kielar AZ, Elsayes KM, Bashir MR, et al. Liver imaging reporting and data system (LI-RADS) version 2018: imaging of hepatocellular carcinoma in at-risk patients. *Radiology* 2018;289:816-830
12. Cerny M, Bergeron C, Billiard JS, Murphy-Lavallée J, Olivié D, Bérubé J, et al. LI-RADS for MR imaging diagnosis of hepatocellular carcinoma: performance of major and ancillary features. *Radiology* 2018;288:118-128
13. Elsayes KM, Kielar AZ, Elmohr MM, Chernyak V, Masch WR, Furlan A, et al. White paper of the Society of Abdominal Radiology hepatocellular carcinoma diagnosis disease-focused panel on LI-RADS v2018 for CT and MRI. *Abdom Radiol (NY)* 2018;43:2625-2642
14. Cerny M, Chernyak V, Olivié D, Billiard JS, Murphy-Lavallée J, Kielar AZ, et al. LI-RADS version 2018 ancillary features at MRI. *Radiographics* 2018;38:1973-2001
15. Zech CJ, Ba-Ssalamah A, Berg T, Chandarana H, Chau GY, Grazioli L, et al. Consensus report from the 8th International Forum for Liver Magnetic Resonance Imaging. *Eur Radiol* 2019 Aug 5 [Epub ahead of print]. https://doi.org/10.1007/s00330-019-06369-4
16. Li J, Wang J, Lei L, Yuan G, He S. The diagnostic performance of gadoxetic acid disodium-enhanced magnetic resonance imaging and contrast-enhanced multi-detector computed tomography in detecting hepatocellular carcinoma: a meta-analysis of eight prospective studies. *Eur Radiol* 2019 Jun 27 [Epub ahead of print]. https://doi.org/10.1007/s00330-019-06294-6
17. Korean Society of Abdominal Radiology. Diagnosis of hepatocellular carcinoma with gadoxetic acid-enhanced MRI: 2016 consensus recommendations of the Korean Society of Abdominal Radiology. *Korean J Radiol* 2017;18:427-443
18. Imai Y, Katayama K, Hori M, Yakushijin T, Fujimoto K, Itoh T, et al. Prospective comparison of Gd-EOB-DTPA-enhanced MRI with dynamic CT for detecting recurrence of HCC after radiofrequency ablation. *Liver Cancer* 2017;6:349-359
19. Roberts LR, Sirlin CB, Zaiem F, Almasri J, Prokop LJ, Heimbach JK, et al. Imaging for the diagnosis of hepatocellular carcinoma: a systematic review and meta-analysis. *Hepatology* 2018;67:401-421
20. Hajian-Tilaki K. Sample size estimation in diagnostic test studies of biomedical informatics. *J Biomed Inform* 2014;48:193-204
21. Pencina MJ, D'Agostino RB Sr, D'Agostino RB Jr, Vasan RS. Evaluating the added predictive ability of a new marker: from area under the ROC curve to reclassification and beyond. *Stat Med* 2008;27:157-172; discussion 207-212
22. Liu X, Jiang H, Chen J, Zhou Y, Huang Z, Song B. Gadoxetic acid disodium-enhanced magnetic resonance imaging outperformed multidetector computed tomography in diagnosing small hepatocellular carcinoma: a meta-analysis. *Liver Transpl* 2017;23:1505-1518
23. Choi SH, Lee SS, Kim SY, Park SH, Park SH, Kim KM, et al. Intrahepatic cholangiocarcinoma in patients with cirrhosis: differentiation from hepatocellular carcinoma by using gadoxetic acid-enhanced MR imaging and dynamic CT. *Radiology* 2017;282:771-781
24. Chen N, Motosugi U, Morisaka H, Ichikawa S, Sano K, Ichikawa T, et al. Added value of a gadoxetic acid-enhanced hepatocyte-phase image to the LI-RADS system for diagnosing hepatocellular carcinoma. *Magn Reson Med Sci* 2016;15:49-59
25. Joo I, Lee JM, Lee DH, Ahn SJ, Lee ES, Han JK. Liver imaging reporting and data system v2014 categorization of hepatocellular carcinoma on gadoxetic acid-enhanced MRI: comparison with multiphasic multidetector computed tomography. *J Magn Reson Imaging* 2017;45:731-740
26. Kim YN, Song JS, Moon WS, Hwang HP, Kim YK. Intra-individual comparison of hepatocellular carcinoma imaging features on contrast-enhanced computed tomography, gadopentetate dimeglumine-enhanced MRI, and gadoxetic acid-enhanced MRI. *Acta Radiol* 2018;59:639-648
27. Fraum TJ, Tsai R, Rohe E, Ludwig DR, Salter A, Nalbantoglu I, et al. Differentiation of hepatocellular carcinoma from other hepatic malignancies in patients at risk: diagnostic performance of the liver imaging reporting and data system version 2014. *Radiology* 2018;286:158-172
28. Kim MJ, Lee S, An C. Problematic lesions in cirrhotic liver mimicking hepatocellular carcinoma. *Eur Radiol* 2019;29:5101-5110
29. Kim YY, Kim MJ, Kim EH, Roh YH, An C. Hepatocellular carcinoma versus other hepatic malignancy in cirrhosis: performance of LI-RADS version 2018. *Radiology* 2019;291:72-80
30. Lee HS, Kim MJ, An C. How to utilize LR-M features of the LI-RADS to improve the diagnosis of combined hepatocellular-cholangiocarcinoma on gadoxetate-enhanced MRI? *Eur Radiol* 2019;29:2408-2416
31. Ludwig DR, Fraum TJ, Cannella R, Ballard DH, Tsai R, Naeem M, et al. Hepatocellular carcinoma (HCC) versus non-HCC: accuracy and reliability of liver imaging reporting and data system v2018. *Abdom Radiol (NY)* 2019;44:2116-2132
32. Ronot M, Fouque O, Esvan M, Lebigot J, Aubé C, Vilgrain V. Comparison of the accuracy of AASLD and LI-RADS criteria for the non-invasive diagnosis of HCC smaller than 3 cm. *J Hepatol* 2018;68:715-723
33. Becker AS, Barth BK, Marquez PH, Donati OF, Ulbrich EJ, Karlo C, et al. Increased interreader agreement in diagnosis of hepatocellular carcinoma using an adapted LI-RADS algorithm. *Eur J Radiol* 2017;86:33-40
34. Barth BK, Donati OF, Fischer MA, Ulbrich EJ, Karlo CA, Becker

A, et al. Reliability, validity, and reader acceptance of LI-RADS—An in-depth analysis. *Acad Radiol* 2016;23:1145-1153
35. Fowler KJ, Tang A, Santillan C, Bhargavan-Chatfield M, Heiken J, Jha RC, et al. Interreader reliability of LI-RADS version 2014 algorithm and imaging features for diagnosis of hepatocellular carcinoma: a large international multireader study. *Radiology* 2018;286:173-185

https://doi.org/10.3348/kjr.2019.0363